Antiviral Research 236 (2025) 106113

Contents lists available at ScienceDirect

Antiviral Research

journal homepage: www.elsevier.com/locate/antiviral

25R,26-hydroxycholesterol and an oxysterol synthetic analog inhibit Varicella zoster Virus replication

Andrea Civra [a,*], Matteo Costantino [a], Domiziana Porporato [a,b], Rachele Francese [a], Manuela Donalisio [a], Giuseppe Poli [a], Maura Marinozzi [c,**], David Lembo [a,***]

[a] Department of Clinical and Biological Sciences, University of Turin, Orbassano, Turin, 10043, Italy
[b] National PhD Programme in One Health Approaches to Infectious Diseases and Life Science Research, Department of Public Health, Experimental and Forensic Medicine, University of Pavia, Pavia, 27100, Italy
[c] Department of Pharmaceutical Sciences, University of Perugia, Perugia, 06123, Italy

ARTICLE INFO

Keywords:
Varicella zoster virus
Oxysterols
Synthetic derivatives
Glycoproteins

ABSTRACT

Varicella-zoster Virus (VZV) is a relevant pathogen belonging to the *herpesviridiae* family. Primary VZV infection causes chickenpox, and results in latent infection of sensory ganglia. Later in life, VZV can reactivate causing herpes zoster (HZ), which can be associated with severe complications in immunocompromised individuals. Currently, the available antivirals used to treat VZV infection target the DNA replication stage; however, resistance to these drugs has been reported in both immunocompromised and immunocompetent patients. For this reason, the identification of new antiviral molecules against VZV infection is a priority. Recently our research group demonstrated that the endogenous oxysterol 25R,26-hydroxycholesterol (25R,26OHC, more commonly named 27-hydroxycholesterol) and an oxysterol synthetic analog named PFM067 inhibit herpes simplex virus (HSV) replication. In this study we explored the antiviral activity of 25-hydroxycholesterol (25OHC), 25R,26OHC, and PFM067 against VZV. We demonstrated that 25R,26OHC and PFM067 exert antiviral activity against VZV with an EC_{50} in the low micromolar range and are able to significantly reduce the area of the viral plaques. Moreover, 25R,26OHC and PFM067 can inhibit the egress of viral glycoprotein gE from the cis-Golgi compartment, similarly to what demonstrated by our group for HSV-2. Additionally, we show that 25R,26OHC and PFM067 act synergistically when used in combination with acyclovir (ACV). The promising antiviral activity of 25R,26OHC and PFM067, along with their different mechanism of action compared to ACV, makes these molecules suitable candidates for further investigation of the molecular target of oxysterols.

Varicella-zoster Virus (VZV) is a double-stranded DNA virus belonging to the family of *herpesviridae*. In susceptible immunocompetent individuals, primary infection by VZV causes chickenpox, which typically manifests as a self-limiting skin blistering rash preceded by flu-like symptoms. During primary infection, VZV can reach sensory ganglia, establishing a lifelong latent infection; in some cases, VZV reactivates and causes herpes zoster (HZ; also known as shingles), which typically manifests with a unilateral vesicular rash, pain (post-herpetic neuralgia [PHN]), neurological complications, and, occasionally, vasculopathy. More than 95% of adults are seropositive for VZV and are at risk of developing HZ (Johnson, 2010).

Immunocompromised individuals (e.g. hematopoietic stem cell transplant [HSCT] recipients, solid organ transplant recipients, and patients with hematological malignancies, solid tumors, or patients with

Abbreviations: (VZV), Varicella Zoster virus; (HSV-2), herpes simplex virus type 2; (25OHC), 25-hydroxycholesterol; (25*R*,26OHC), 25*R*,26-hydroxycholesterol; (EC_{50}), 50% effective concentration; (EC_{90}), 90% effective concentration; (CC_{50}), 50% cytotoxic concentration; (SI), selectivity index; (CPE), cytopathic effect; (EtOH), ethanol; (DMSO), dimethyl sulfoxide; (DMEM), Dulbecco's Modified Eagle Medium; (FBS), fetal bovine serum; (PFU), plaque-forming units; (MOI), multiplicity of infection; (ANOVA), analysis of variance; (SEM), standard error of the mean.

* Corresponding author.
** Corresponding author.
*** Corresponding author.
E-mail addresses: andrea.civra@unito.it (A. Civra), m.costantino@unito.it (M. Costantino), domiziana.porporato@unito.it, domiziana.porporato01@universitadipavia.it (D. Porporato), rachele.francese@unito.it (R. Francese), manuela.donalisio@unito.it (M. Donalisio), giuseppe.poli@unito.it (G. Poli), maura.marinozzi@unipg.it (M. Marinozzi), david.lembo@unito.it (D. Lembo).

https://doi.org/10.1016/j.antiviral.2025.106113
Received 15 October 2024; Received in revised form 11 February 2025; Accepted 12 February 2025
Available online 13 February 2025

acquired immunodeficiency syndrome [AIDS]) are at increased risk of HZ and HZ complications (e.g. PHN, disseminated HZ, HZ ophthalmicus, and HZ requiring hospitalization).

Given the high prevalence of VZV infections, prevention is of utmost importance. Currently, only vaccines and passive immunoprophylaxis against VZV are available. Vaccines to prevent HZ approved for use in older adults include live-attenuated VZV vaccine (zoster vaccine live, ZVL) and an adjuvanted recombinant zoster vaccine (RZV) based on the VZV glycoprotein E (gE) (Harbecke et al., 2021).

All the currently available antiviral drugs to treat VZV infection target the DNA replication stage, by means of different mechanisms (Shiraki et al., 2021). In this regard, a particular concern is raised by the emergence of resistance toward the first-line drug for the treatment of VZV infection (i.e. the deoxyguanosine analog acyclovir [ACV]), in

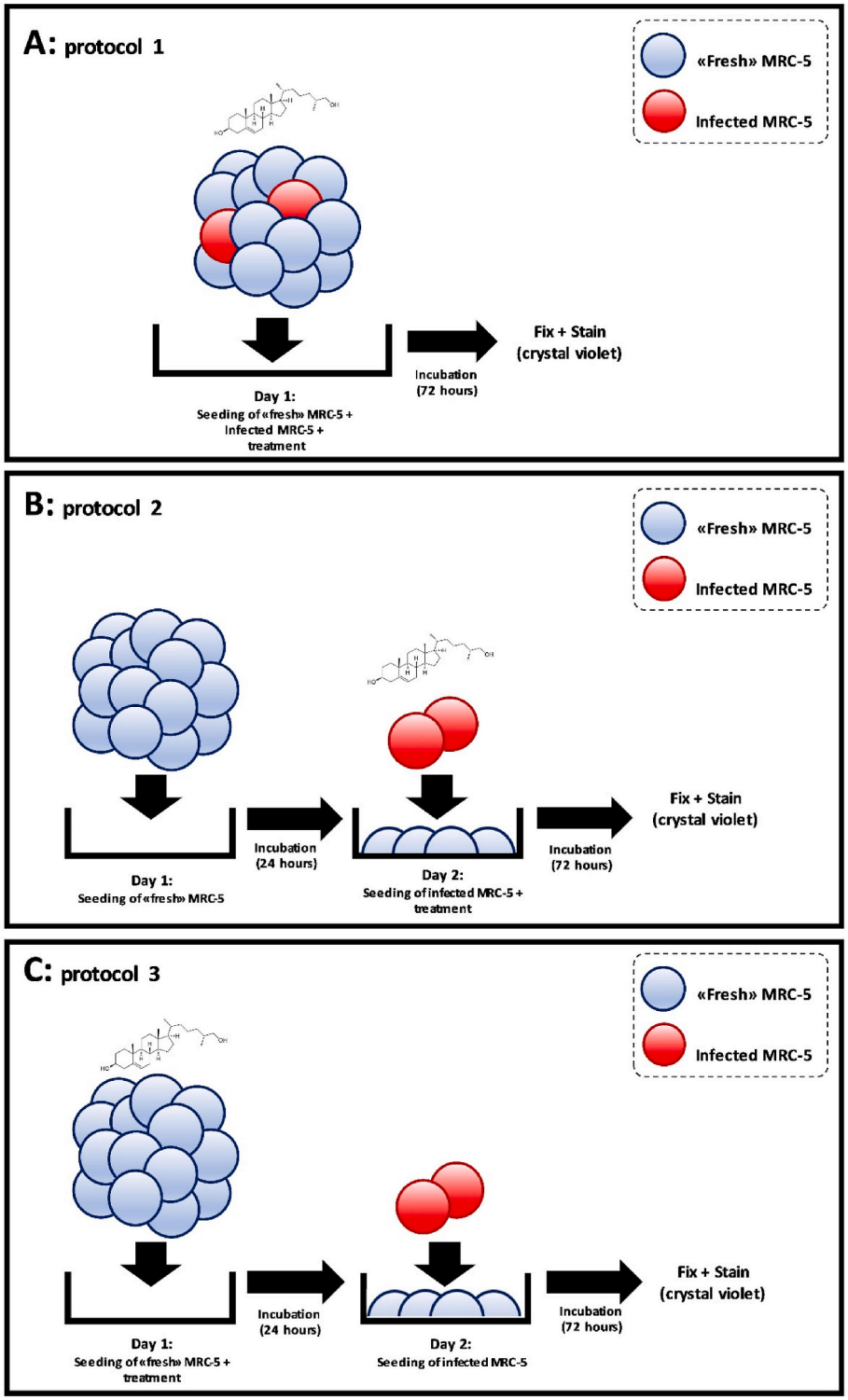

Fig. 1. Schematic representation of the three protocols used in the antiviral assays (panels A, B, and C). The light blue circles represent freshly detached MRC-5 cells, while the red circles represent cell-associated VZV. (For interpretation of the references to colour in this figure legend, the reader is referred to the Web version of this article.)

particular in immunocompromised patients with persistent VZV infections (Andrei and Snoeck, 2021); in particular, antiviral resistance was found in 27% of onco-hematological patients with persistent VZV infection, including patients that progressed to severe retinal or cerebral infection (van der Beek et al., 2013). ACV resistance was also documented in a case of VZV keratitis in an immunocompetent patient (Gueudry et al., 2013). For these reasons, it is crucial to identify and develop novel antiviral molecules with innovative targets and mechanisms of action to treat VZV infection.

Oxysterols are a class of cholesterol-derived molecules of both enzymatic and non-enzymatic origin; among enzymatic oxysterols, 25-hydroxycholesterol (25OHC) and 25R,26-hydroxycholesterol (25R,26OHC; more commonly referred to as 27-hydroxycholesterol) have raised particular interest as they act as broad-spectrum antivirals, against both enveloped and non-enveloped viruses (Blanc et al., 2013; Liu et al., 2013; Lembo et al., 2016).

These molecules act as host-targeting antivirals by modifying the membrane composition of intracellular organelles, and their effect on viral replicative cycle differs depending on virus-host interactions; in particular, 25OHC and/or 25R,26OHC inhibit virus-cell fusion of several enveloped viruses (e.g. human immunodeficiency virus, and Ebola virus), the entry of human rotavirus, and the genome replication of human rhinovirus (Liu et al., 2013; Civra et al., 2014, 2018). In this regard, our group has recently shown that 25R,26OHC, along with a panel of oxysterol synthetic analogs named PFMs, inhibit the HSV-2 replication, by hampering the export of viral fusogenic glycoproteins from the Golgi compartment (Civra et al., 2023).

In this study, we further explore the spectrum of activity of 25OHC and 25R,26OHC against herpesviridae, along with the N,N-dimethyl 3β-hydroxychol-5-en-24-amide PFM067, i.e. the oxysterol synthetic analog that showed the highest efficacy against HSV-2, by investigating their antiviral efficacy against VZV. Briefly, VZV was cultured on human lung fibroblast MRC-5 (ATCC® CCL-171) as described in the supplementary material and data, at a ratio of 1 infected cell to 8 uninfected cells (Grose and Brunel, 1978).

The antiviral efficacy of 25OHC, 25R,26OHC or PFM067 against cell-associated VZV was determined by plaque reduction assay, by using three different protocols (Fig. 1, panels A, B, and C). Briefly, for protocol 1 (Fig. 1A), MRC-5 cells were detached with 0.05% trypsin-EDTA and counted. At the same time, cell-associated virus was quickly thawed and centrifuged at 1200 rpm for 10 min to remove the DMSO and resuspended with DMEM supplemented with 20% FBS. A suspension containing 50,000 MRC-5/ml and cell-associated virus (ca. 50 PFU/ml) was prepared and seeded in 24-well plates in presence of serial dilutions of 25OHC, 25R,26OHC, or PFM067 (ranging from 0.07 μM to 5.6 μM), or ACV (ranging from 0.2 μM to 16.7 μM). Each sample was prepared in triplicate. For 25OHC and 25R,26OHC, control untreated samples (100% of infectivity) were prepared by treating cells with culture medium supplemented with equal volumes of ethanol, corresponding to 0.19% (v/v) to 0.0023% (v/v). For PFM067, control samples were prepared by treating cells with culture medium supplemented with equal volumes of ethanol, ranging to 0.04% (v/v) to 0.0006% (v/v). Alternatively, for protocol 2 (Fig. 1B) MRC-5 cells were plated in 24-well plates at 50,000 cells/well. After 24 h, cell-associated virus was diluted to reach a MOI (multiplicity of infection) of 0.005 PFU/cell and used to infect cell monolayers, in presence of serially diluted 25OHC, 25R,26OHC, PFM067 or ACV. In a third protocol (Fig. 1C), freshly trypsinized MRC-5 cells were seeded in 24-well plates at 50,000 cells/well, in presence of serial dilutions of 25OHC, 25R,26OHC, PFM067 or ACV; after 24 h, cell-associated virus was added on preplated/pretreated cell monolayers at a MOI of 0.005 PFU/cell. For all these protocols, the cells were then incubated at 37 °C for 72 h. Infected monolayers were then fixed and stained with crystal violet (Sigma, St. Louis, Mo.). The number of plaques was counted, and viral titers were expressed in terms of plaque forming units per ml (PFU/ml). In parallel, the effect of 25OHC, 25R,26OHC, PFM067 or ACV on MRC-5 viability was assessed by tetrazolium salt-based cell viability assays, as described in supplementary materials. Where possible, half-maximal antiviral effective concentration (EC_{50}), 90% effective concentration (EC_{90}), 50% cytotoxic concentration (CC_{50}), were calculated as described in supplementary materials. Selectivity indexes (SIs, resulting from the ratio between CC_{50} and EC_{50}) were also calculated, in order to assess the distance between effective and cytotoxic concentrations. The results shown in Table 1 and depicted in Fig. 2A demonstrate that 25R,26OHC inhibits VZV infectivity with an EC_{50} in the low micromolar range (0.33 μM), and an SI > 151.51, when the treatment was performed during the seeding of both fresh MRC-5 and cell-associated VZV (indicated as Protocol 1). Notably, in the same experimental setting, 25R,26OHC was significantly ($p_{Ftest}<0.001$) more effective than ACV (EC_{50} = 9.72 μM; Table 1, Fig. 2D).

25R,26OHC shows a comparable level of efficacy (EC_{50} = 0.54 μM) even if the treatment is performed according to Protocol 2, i.e. during infection with cell-associated VZV on pre-seeded MRC-5 cells (Table 1, Fig. 2A).

Conversely, when the treatment is performed during the sowing of fresh MRC-5 only (i.e., 24 h before infection with the cell-associated virus; Protocol 3), 25R,26OHC shows an EC_{50} equal to 1.23 μM (maintaining the ability to inhibit the infection up to a maximum of 100%; Table 1, Fig. 2A), while ACV totally loses the ability to inhibit viral replication (Table 1; Fig. 2D). These data are particularly relevant if contextualized in the pathogenesis of VZV infection, as they demonstrate that 25R,26OHC is effective at low micromolar concentrations, therefore lower than those which, based on literature data, exert cytotoxicity on neuronal cells (Wang et al., 2016; Nakazawa et al., 2017; Jamadagni and Patten, 2019).

Interestingly, in none of the tested experimental settings 25OHC showed a relevant antiviral activity (Table 1; Fig. 2B); this data is peculiar since 25OHC and 25R,26OHC usually show comparable efficacy in studies in which their antiviral activity is tested in parallel, with 25OHC slightly more effective than 25R,26OHC (Civra et al., 2014, 2018, 2022). More interestingly, 25OHC was more cytotoxic than 25R,26OHC, with CC_{50}s ranging from 3.4 μM to 17.1 μM, and SIs ranging from 8.5 to 8.9. This result is consistent with previous data from our group, showing the highest cytotoxic effect of 25OHC on HeLa cells respectively to 25R,26OHC (Civra et al., 2022).

PFM067 showed an efficacy profile similar to the one of 25R,26OHC (Fig. 2C) for all protocols tested, showing the lowest EC50s for Protocols 1 and 2 (0.30 μM and 0.21 μM, respectively; Table 1) and the highest one for Protocol 3 (2.04 μM; Table 1). Notably, PFM067 has a less promising SIs than 25R,26OHC, ranging from 9.0 to >24.5, depending on the protocol used (Table 1).

As a further investigation of the antiviral efficacy of 25R,26OHC, 25OHC, and PFM067, we performed a second set of experiments, measuring the dimensions of viral plaques at 72 h post infection. In order to assess the dimensions of viral plaques, fresh MRC-5 and cell-associated virus were treated during the seeding process, as previously described. After an incubation of 72 h at 37 °C, cells were washed with phosphate-buffered saline (PBS), and fixed with cold acetone-methanol (50:50). Cells were then permeabilized with Triton X-100 0.1% in PBS, and incubated with the VZV-specific monoclonal antibody. After three quick washes with PBS, the secondary peroxidase-conjugated antibody was added. Finally, after three more washes with PBS, 3, 3′ diaminobenzidine tetrahydrochloride (DAB Substrate; 11718096001, Merck Life Science Srl, Milan, Italy) was added. 13 to 30 images of viral plaques were captured for each sample under inverted microscope; the dimensions of the plaques were assessed with ImageJ Software (U. S. National Institutes of Health, Bethesda, Maryland, USA). As shown respectively in Fig. 3A and B, 25R,26OHC and PFM067 are able to significantly ($p_{ANOVA} < 0.0001$) reduce the area of the viral plaques down to a concentration of 0.2 μM. In contrast, 25OHC slightly reduces VZV plaque dimensions at 1.9 μM (Fig. 3B), but the difference with the untreated control is not significant ($p_{ANOVA} > 0.05$); moreover, when

Table 1
Anti-VZV activity of 25OHC, 25R,26OHC, and ACV.

Treatment	Protocol	EC50[a] (μM) – 95% C.I.[b]	EC90[c] (μM) – 95% C.I.	CC50[d] (μM) – 95% C.I.	SI[e]
25R,26OHC	1[f]	0.33 (0.23–0.47)	0.95 (0.68–1.35)	>50	>151.51
	2[g]	0.54 (0.33–0.86)	2.59 (0.90–7.40)	>50	>92.59
	3[h]	1.23 (0.74–1.98)	3.26 (1.22–10.65)	>50	>40.65
25OHC	1	0.40 (0.22–0.73)	n.a.	3.39 (2.80–4.10)	8.48
	2	0.38 (0.22–0.65)	n.a.	3.39 (2.80–4.10)	8.92
	3	n.a.	n.a.	17.13 (13.22–22.20)	n.a.
PFM067	1	0.30 (0.25–0.35)	1.05 (0.73–1.50)	2.70 (2.40–3.00)	9.00
	2	0.21 (0.16–0.28)	0.50 (0.22–1.15)	2.70 (2.40–3.00)	12.86
	3	2.04 (1.29–3.23)	9.82 (2.86–33.68)	>50	>24.51
ACV	1	9.72 (7.25–13.02)	>16.7	>1350	>138.88
	2	1.25 (0.82–1.92)	3.99 (1.64–9.71)	>1350	>1080.00
	3	n.a.	n.a.	>1350	n.a.

n.a. not assessable.
[a] EC50 half-maximal effective concentration.
[b] CI confidence interval.
[c] EC90 90% effective concentration.
[d] CC50 half maximal cytotoxic concentration.
[e] SI selectivity index = CC50/EC50.
[f] Treatment during infection.
[g] Treatment after seeding of fresh cells.
[h] Treatment 24 h before infection.

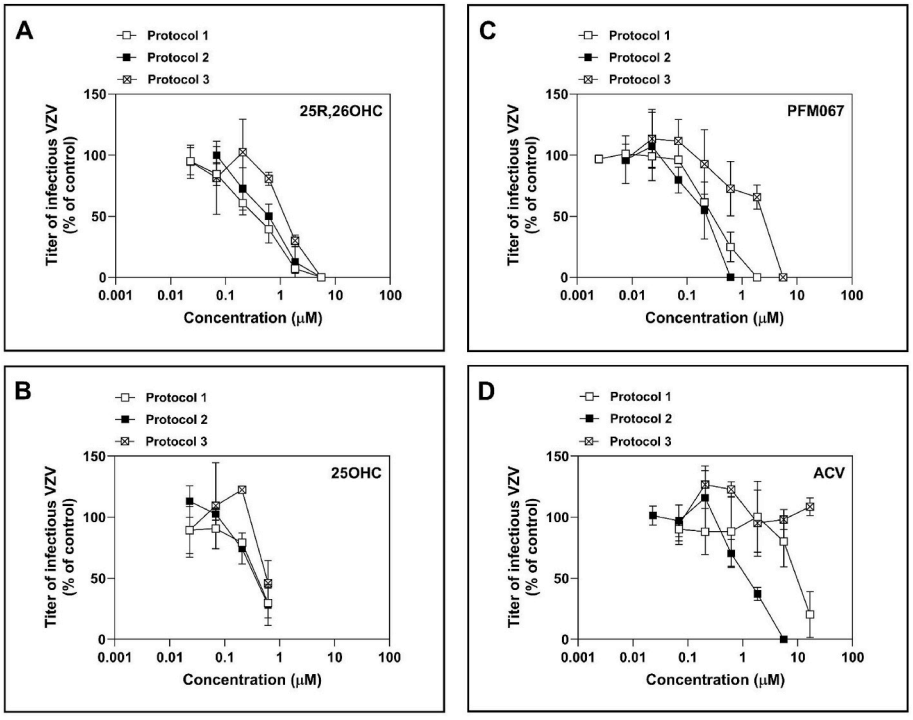

Fig. 2. Anti-VZV activity of 25R,26OHC (panel A), 25OHC (panel B), PFM067 (panel C) and ACV (panel D) on MRC-5 cells. In each panel three dose-response curves are represented, corresponding to three different treatment/infection protocols. Protocol 1: suspensions of freshly trypsinized MRC-5 and cell associated virus were seeded in presence of serial dilutions of 25OHC, 25R,26OHC, or ACV. Protocol 2: suspensions of freshly trypsinized MRC-5 were seeded in 24-well plates. After 24 h, cell-associated virus was added in presence of serial dilutions of 25OHC, 25R,26OHC, or ACV. Protocol 3: suspensions of freshly trypsinized MRC-5 were seeded in 24-well plates in presence of serially dilutions of 25OHC, 25R,26OHC, or ACV. After 24 h, cell-associated virus was added. Viral infections were assessed at 72 h post-infection, by plaque counting under inverted microscope. The percentage infection was calculated by comparing treated and untreated wells. The results are means and SD for triplicates.

tested at 5.6 μM, 25OHC is cytotoxic. ACV significantly ($p_{ANOVA} < 0.01$) reduces the area of the plaques only when used at a concentration of 5.6 μM (Fig. 3C).

In a previous study, our group demonstrated that 25R,26OHC and PFM067 were able to inhibit the release of HSV-2 structural glycoproteins from the Golgi and therefore showed a different antiviral mechanism of action compared to ACV (Civra et al., 2023). To investigate whether 25R,26OHC and PFM067 had the same effect on VZV replication, we performed immunofluorescence experiments to identify the intracellular localization of the VZV gE glycoprotein. Briefly, MRC-5 cells were treated with 25R,26OHC, PFM067, or ACV at respective EC_{90}s and infected by using protocol 1 experimental design. After 72 h,

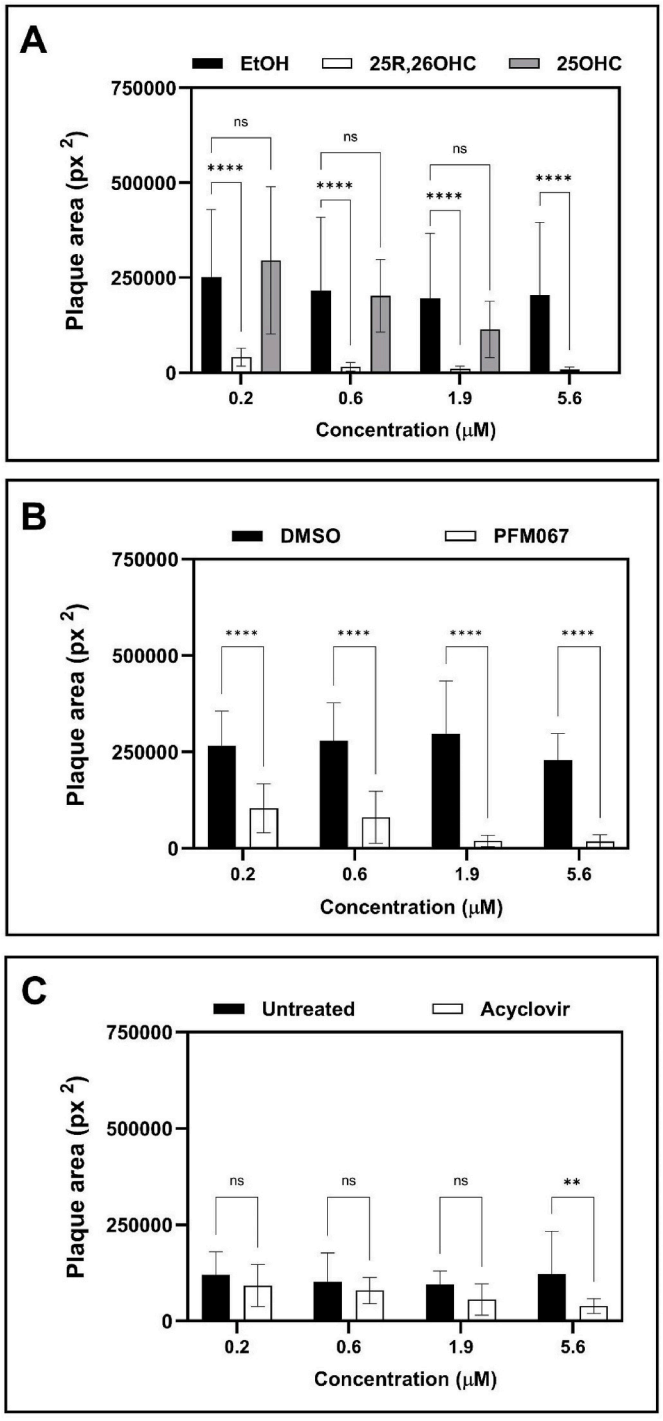

Fig. 3. Effect of 25R,26OHC, 25OHC (both in panel A), PFM067 (panel B), or ACV (panel C) on VZV plaques areas. Suspensions of freshly trypsinized MRC-5 cells and cell-associated virus were seeded in presence of serial dilutions of molecules. Untreated controls were prepared by treating cells with equal volumes of ethanol, DMSO, or culture medium (respectively for 25R,26OHC and 25OHC, PFM067, or ACV). After 72 h, cells were fixed and viral plaques were stained by indirect immunocytochemistry. Images of viral plaques were captured for each sample under inverted microscope; the dimensions of the plaques were assessed with ImageJ Software (U. S. National Institutes of Health, Bethesda, Maryland, USA). On y axis, plaque areas are expressed as squared pixels (px^2). $^{**}p_{ANOVA} < 0.01$; $^{****}p_{ANOVA} < 0.0001$.

VZV-infected cell monolayers were fixed with 4% paraformaldehyde for 20 min at room temperature, and stained with VZV gE- and GM130-specific antibodies, according to the protocol described in the supplementary materials.

The results reported in Fig. 4A show that gE colocalizes with a cis-Golgi marker (i.e. GM130) and is widely dispersed in the cytoplasm of non-treated infected cells. By contrast, in cells treated with 25R,26OHC or PFM067 (Fig. 4B and D) gE strictly localizes in the cis-Golgi compartment. By contrast, when cells are treated with the highest non-cytotoxic concentration of 25OHC, the intracellular localization pattern of gE is similar to the one assessed in the non-treated control (Fig. 4C); these data, taken together with the fact that 25OHC does not reduce significantly the dimensions of VZV plaques (Fig. 3A), suggest that the antiviral effect measured on 25OHC-treated VZV-infected cells (Fig. 2B) was due to a non-specific cytotoxic effect mediated by the molecule. As expected, in ACV-treated cells, gE is not detectable (Fig. 4D).

Taken together, these data show that - similarly to what was seen previously for HSV-2 (Civra et al., 2023) - 25R,26OHC and PFM067 can inhibit the egress of viral glycoproteins from the Golgi compartment; moreover, these results show that both molecules are effective even if the treatment is performed before the infection, strengthening the hypothesis that they function as host-targeting antivirals also against VZV, finally suggesting a different mechanism of action compared to ACV. This consideration is further strengthened by the fact 25R,26OHC or PFM067 reduce the size of VZV plaques more effectively than ACV, similarly to what was seen for the same molecules against HSV-2 (Civra et al., 2023). By contrast, the same data show that 25OHC does not trigger this mechanism of action, and is only partially effective against VZV, while this antiviral activity is at least in part due to its cytotoxicity.

Based on these findings, we explored the ability of 25R,26OHC and PFM067 to act synergistically when used in combination with ACV. The simultaneous effect of ACV and 25R,26OHC, or ACV and PFM067 was analyzed by the isobologram method (50 % isodose) as described previously (Tallarida, 2006). Briefly, fresh MRC-5 cells and cell-associated virus were seeded in 96-well in presence of fixed percentages (20, 60, or 100%) of the half-maximal concentration (EC50) of the first drug (e.g. ACV), and serial dilutions (from 0.02 to 16.7 μM) of the second drug (e.g. 25R,26OHC). The same procedure was carried out inversely for the second drug. After 72 h of incubation at 37 °C, the cells were fixed and subjected to indirect immunoperoxidase staining as described previously. As depicted in Table 1S and Fig. 1S, when 25R,26OHC or PFM067 are used at sub-optimal concentrations in combination with ACV, they both significantly ($p_{ANOVA} < 0.001$) improve the efficacy of the nucleoside analogue. In order to test the effect of the combined treatment of ACV and 25R,26OHC, an isobologram-based analysis was performed. As depicted in Fig. 5, the interaction between ACV and 25R,26OHC and the one between ACV and PFM067 were significantly synergistic. The fact that 25R,26OHC synergizes with ACV suggests a virtuous interaction between the mechanisms of action of the two molecules: working on this hypothesis, it may be interesting to investigate the molecular target of 25R,26OHC, in order to understand the molecular reasons for the improvement in efficacy of the ACV. This could be especially important for treating ACV-resistant VZV infections.

In conclusion, in this study we demonstrated that the physiological oxysterol 25R,26OHC and the synthetic oxysterol analog PFM067 (A) are able to inhibit VZV replication by blocking the export of the viral glycoprotein gE from the cis-Golgi and (B) enhance the antiviral activity of ACV. These data, together with further evidences previously obtained by our group demonstrating that 25R,26OHC and PFM067 have a similar mechanism of action against HSV (Civra et al., 2023), provide a solid rationale to further non-clinical *in vivo* studies. In this sense, it will be necessary to explore the ADME profile and the pharmacokinetic properties of 25R,26OHC and PFM067 (in particular their solubility): while the steroidal motif has well-established desirable physicochemical properties (so much to be exploited for the design of bioconjugates;

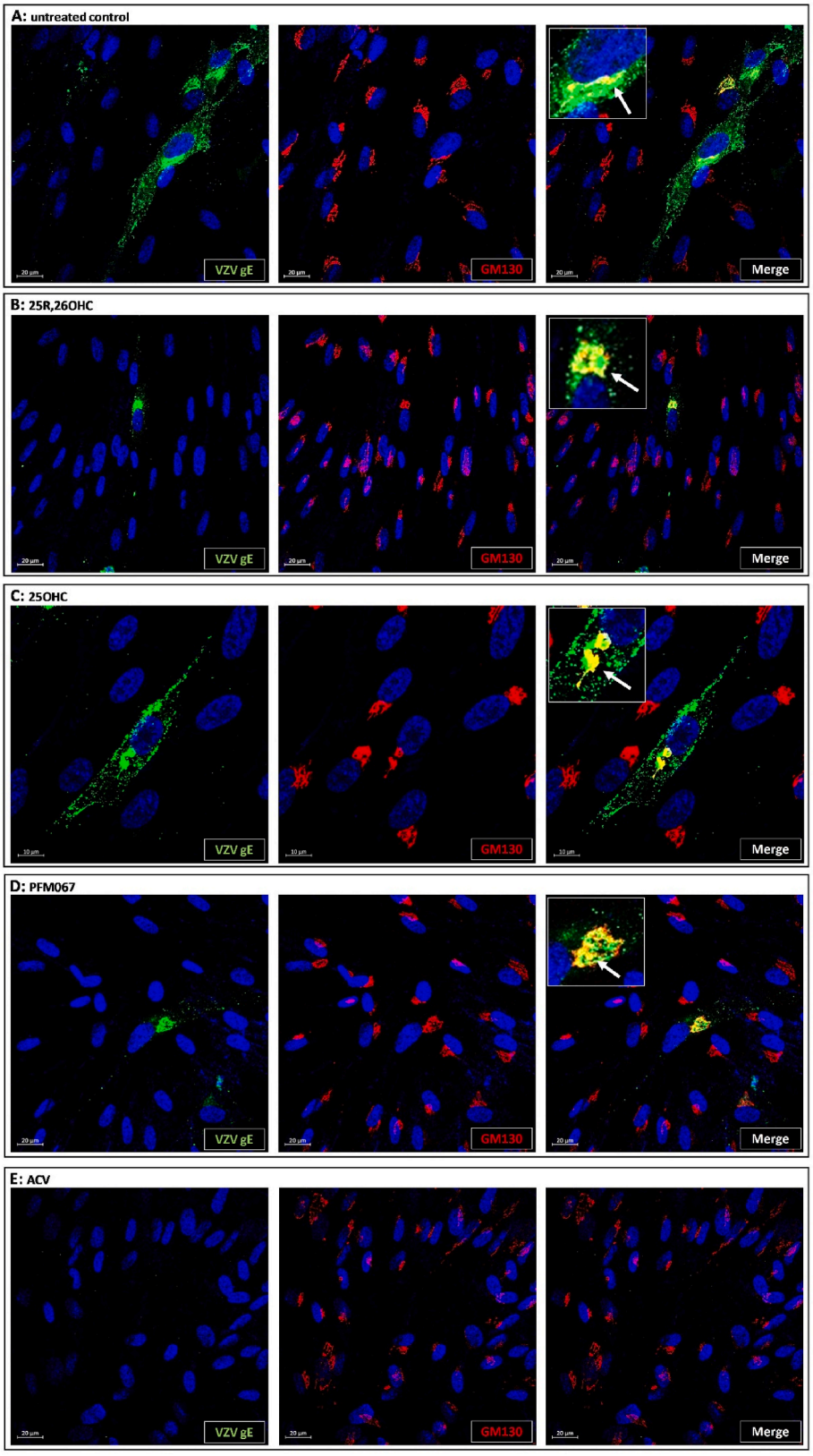

Fig. 4. Indirect immunofluorescence of VZV-infected MRC5 cells. Cells were inoculated and left untreated (panel A) or treated with 25R,26OHC (B), 25OHC (C), PFM067 (D), or ACV (E) at their respective EC90s for 72 h. All monolayers were stained with a GM130-specific antibody (targeting the cis-Golgi compartment), and counterstained with a gE-specific antibody. Nuclea were stained with DAPI. In the appropriate panels, zoomed-in inserts were added; in each insert co-localization between GM130 and gE is indicated with white arrows.

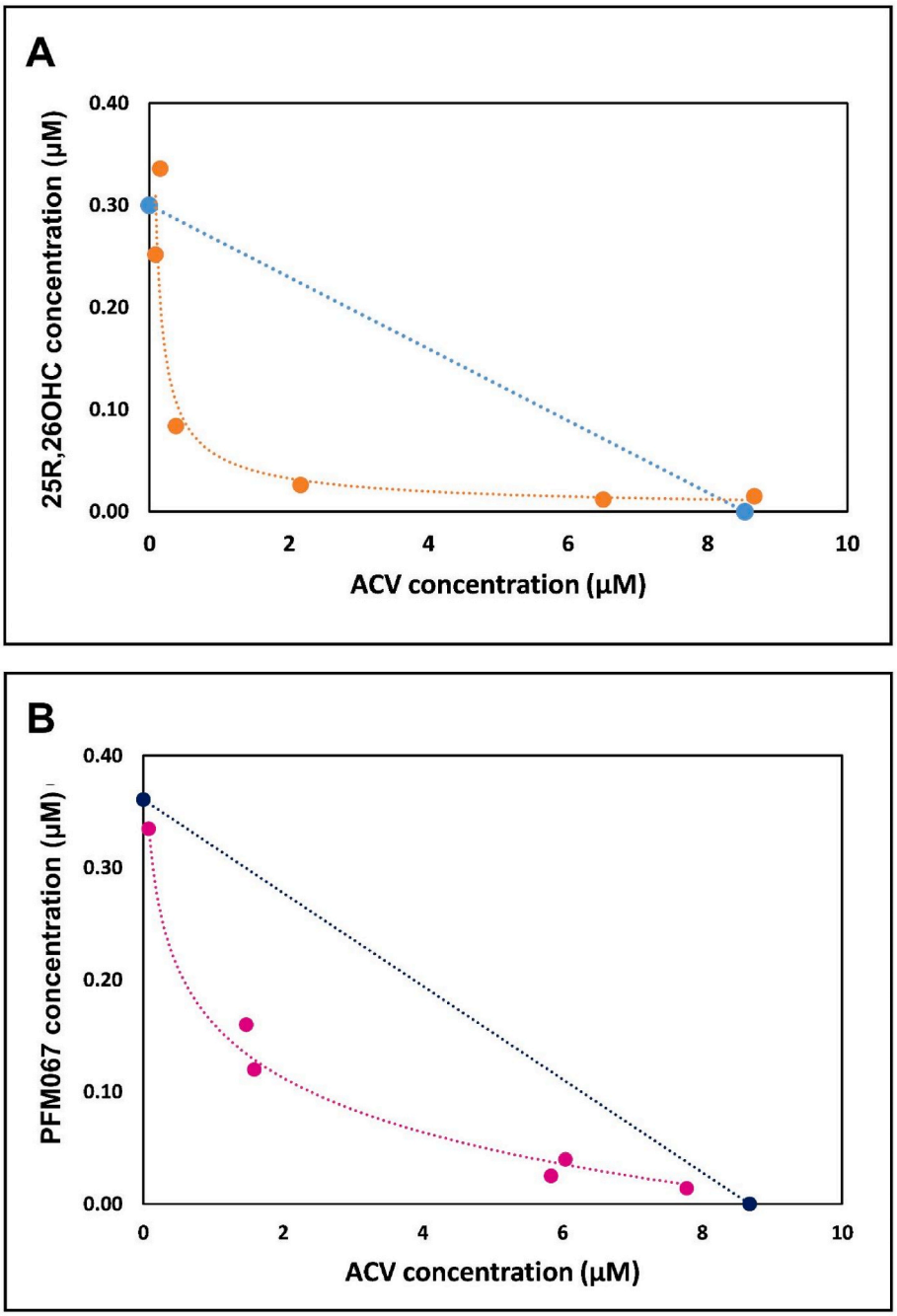

Fig. 5. 25R,26OHC/ACV and PFM067/ACV synergism assessment (panels A and B, respectively) as tested against VZV on MRC-5 cells. The isobolograms (light blue and dark blue lines) result from plotting on x and y axis the EC_{50}s respectively of the ACV and 25R,26OHC, or ACV and PFM067. Each orange or purple dot results respectively from the combination of two concentrations of ACV and 25R,26OHC or ACV and PFM067, each capable to exert 50% inhibition of viral replication. (For interpretation of the references to colour in this figure legend, the reader is referred to the Web version of this article.)

Kawka et al., 2024) we do not exclude the possibility to eventually develop a formulation to improve the pharmacokinetic profile of these molecules. Besides future perspectives, the results obtained in this study suggest that 25R,26OHC and PFM067 should be further studied as prototypes of a new class of anti-herpetic molecules.

Glossary

Oxysterols: a family of molecules derived from cholesterol by means of oxidative processes at the level of the body as well as of the side-chain of the steroid. They are characterized by an oxygenated function, such as hydroxyl, epoxide or ketone moiety, additional to 3β-hydroxyl group.

CRediT authorship contribution statement

Andrea Civra: Writing – original draft, Methodology, Investigation, Conceptualization. **Matteo Costantino:** Investigation, Data curation. **Domiziana Porporato:** Investigation, Data curation. **Rachele Francese:** Writing – review & editing, Investigation. **Manuela Donalisio:** Writing – review & editing, Investigation. **Giuseppe Poli:** Writing – review & editing, Writing – original draft, Supervision, Conceptualization. **Maura Marinozzi:** Writing – review & editing, Supervision, Resources. **David Lembo:** Writing – review & editing, Writing – original draft, Visualization, Supervision, Project administration, Methodology, Investigation, Funding acquisition, Formal analysis, Data curation,

Conceptualization.

Funding

This research was supported by EU funding within the NextGenerationEU-MUR PNRR Extended Partnership initiative on Emerging Infectious Diseases (Project no. PE00000007, INF-ACT).

Declaration of competing interest

The authors declare that they have no known competing financial interests or personal relationships that could have appeared to influence the work reported in this paper.

Appendix A. Supplementary data

Supplementary data to this article can be found online at https://doi.org/10.1016/j.antiviral.2025.106113.

Data availability

Data will be made available on request.

References

Andrei, G., Snoeck, R., 2021. Advances and perspectives in the management of varicella-zoster virus infections. Molecules 26 (4), 1132. https://doi.org/10.3390/molecules26041132.

Blanc, M., et al., 2013. The transcription factor STAT-1 couples macrophage synthesis of 25-hydroxycholesterol to the interferon antiviral response. Immunity 38, 106–118. https://doi.org/10.1016/j.immuni.2012.11.004.

Civra, A., et al., 2023. Identification of oxysterol synthetic analogs as a novel class of late-stage inhibitors of herpes simplex virus 2 replication. Antivir. Res. 215, 105634. https://doi.org/10.1016/j.antiviral.2023.105634.

Civra, A., et al., 2022. 27-Hydroxycholesterol inhibits rhinovirus replication in vitro and on human nasal and bronchial histocultures without selecting viral resistant variants. Antivir. Res. 204, 105368. https://doi.org/10.1016/j.antiviral.2022.105368.

Civra, A., et al., 2018. 25-Hydroxycholesterol and 27-hydroxycholesterol inhibit human rotavirus infection by sequestering viral particles into late endosomes. Redox Biol. 19, 318–330. https://doi.org/10.1016/j.redox.2018.09.003.

Civra, A., et al., 2014. Inhibition of pathogenic non-enveloped viruses by 25-hydroxycholesterol and 27-hydroxycholesterol. Sci. Rep. 4, 7487. https://doi.org/10.1038/srep07487.

Grose, C., Brunel, P.A., 1978. Varicella-zoster virus: isolation and propagation in human melanoma cells at 36 and 32 degrees C. Infect. Immun. 19 (1), 199–203. https://doi.org/10.1128/iai.19.1.199-203.1978.

Gueudry, J., et al., 2013. Acyclovir-resistant varicella-zoster virus keratitis in an immunocompetent patient. J. Clin. Virol. 58 (1), 318–320. https://doi.org/10.1016/j.jcv.2013.04.024.

Harbecke, R., Cohen, J.I., Oxman, M.N., 2021. Herpes zoster vaccines. J. Infect. Dis. 224 (12 Suppl. 2), S429–S442. https://doi.org/10.1093/infdis/jiab387.

Jamadagni, P., Patten, S.A., 2019. 25-hydroxycholesterol impairs neuronal and muscular development in zebrafish. Neurotoxicology 75, 14–23. https://doi.org/10.1016/j.neuro.2019.08.007.

Johnson, R.W., 2010. Herpes zoster and postherpetic neuralgia. Expert Rev. Vaccines 9 (3 Suppl. l), 21–26. https://doi.org/10.1586/erv.10.30.

Kawka, A., et al., 2024. Steroid and bioactive molecule conjugates: improving therapeutic approaches in disease management. Bioorg. Chem. 153, 107933. https://doi.org/10.1016/j.bioorg.2024.107933.

Lembo, D., et al., 2016. Oxysterols: an emerging class of broad spectrum antiviral effectors. Mol. Aspect. Med. 49, 23–30. https://doi.org/10.1016/j.mam.2016.04.003.

Liu, S.-Y., et al., 2013. Interferon-inducible cholesterol-25-hydroxylase broadly inhibits viral entry by production of 25-hydroxycholesterol. Immunity 38, 92–105. https://doi.org/10.1016/j.immuni.2012.11.005.

Nakazawa, T., et al., 2017. Effect of vitamin E on 24(S)-hydroxycholesterol-induced necroptosis-like cell death and apoptosis. J. Steroid Biochem. Mol. Biol. 169, 69–76. https://doi.org/10.1016/j.jsbmb.2016.03.003.

Shiraki, K, Takemoto, M, Daikoku, T., 2021. Emergence of varicella-zoster virus resistance to acyclovir: epidemiology, prevention, and treatment. Expert Rev Anti Infect Ther 19 (11), 1415–1425. https://doi.org/10.1080/14787210.2021.1917992. Epub 2021 Apr 28. PMID: 33853490.

Tallarida, R.J., 2006. An overview of drug combination analysis with isobolograms. J. Pharmacol. Exp. Therapeut. 319 (1), 1–7. https://doi.org/10.1124/jpet.106.104117.

van der Beek, M.T., et al., 2013. Persistence and antiviral resistance of varicella zoster virus in hematological patients. Clin. Infect. Dis. 56 (3), 335–343. https://doi.org/10.1093/cid/cis879.

Wang, H., et al., 2016. The cytotoxicity of 27-hydroxycholesterol in co-cultured SH-SY5Y cells and C6 cells. Neurosci. Lett. 632, 209–217. https://doi.org/10.1016/j.neulet.2016.08.056.